Workshop on Multineutron Clusters in Nuclei and in Stars

(School: May 27 – 31, 2025)

Workshop: June 2 – 6, 2025

ICTP-SAIFR, São Paulo, Brazil

Sub-Coulomb Nuclear Reactions Studied with the Trojan Horse Method

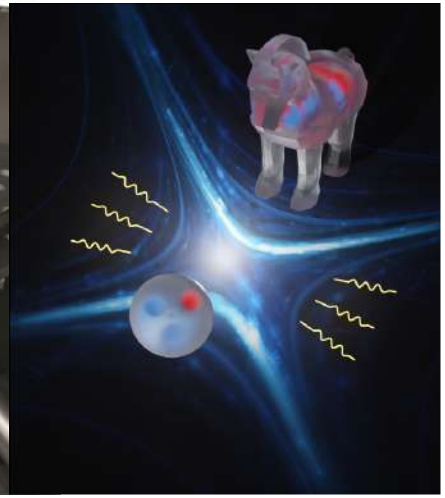

Aurora Tumino

Outline

- Why we need indirect techniques in Nuclear Astrophysics
- Trojan Horse Method (THM)
- Physics cases …

Charged particle cross section measurements at astrophysical energies

σ ~picobarn $\Rightarrow$ Low signal-to-noise ratio due to the Coulomb barrier between the interacting nuclei

measure $\sigma(E)$ over as wide a range as possible, then extrapolate down to E_0!

CROSS SECTION

$$\sigma(E) = \frac{1}{E}\exp(-2\pi\eta)\,S(E)$$

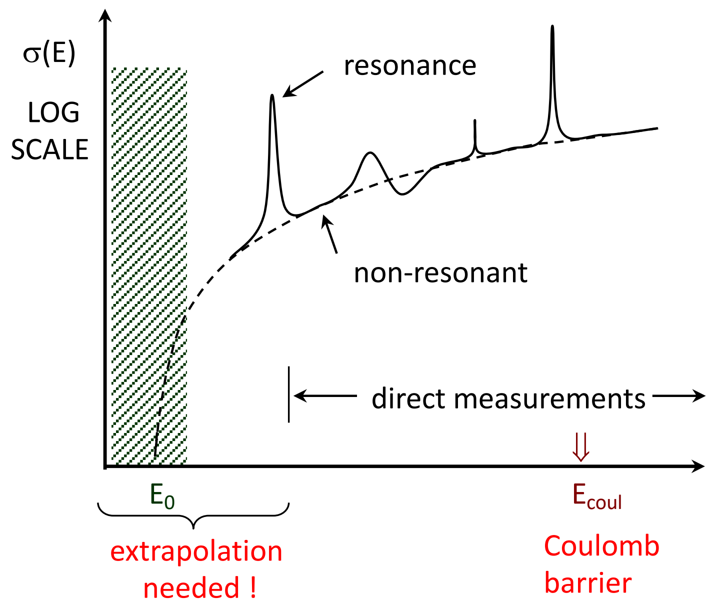

S-FACTOR

$$S(E) = E\sigma(E)\exp(2\pi\eta)$$

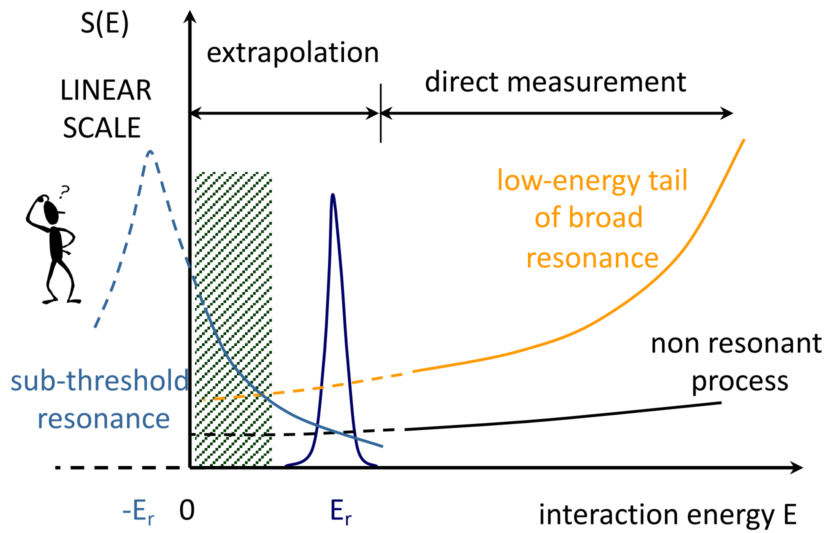

DANGER OF EXTRAPOLATION !

To give you the feeling what low signal-to-noise ratio means

LUNA – Phase I: 50 kV accelerator (1992-2001)

investigate reactions in solar pp chain

R. Bonetti et al.: Phys. Rev. Lett. 82 (1999) 5205

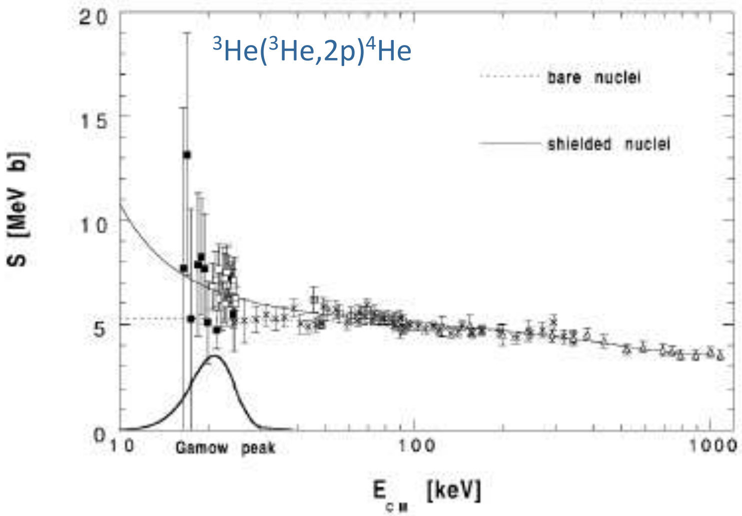

@ lowest energy:

σ ~ 20 fb → 1 count/month

C. Casella et al.: Nucl. Phys. A706 (2002) 203-216

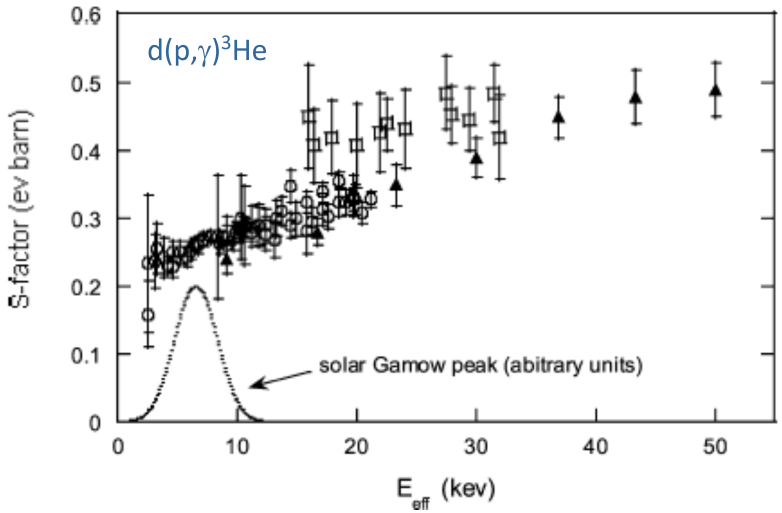

@ lowest energy:

σ ~ 9 pb → 50 counts/day

only two reactions studied directly at the Gamow peak

… intrinsic limitation at astrophysical energies → → → → Electron Screening

S(E) experimental enhancement due to the electron screening $S(E)_s = S(E)_b \exp(\pi\eta U_e/E)$

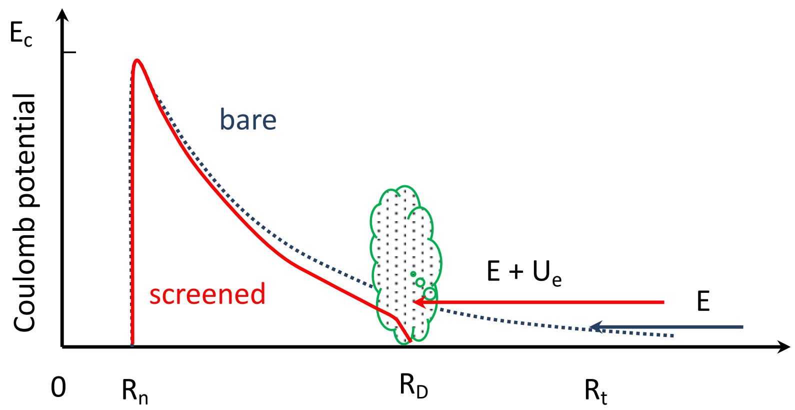

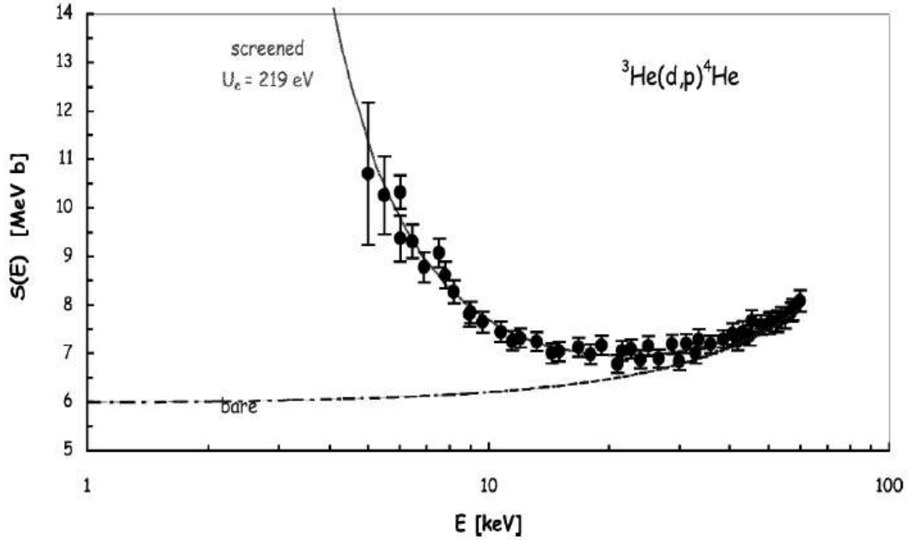

In astrophysical plasma:

- the screening, due to free electrons in plasma, can be different
→ we need $S(E)_b$ to evaluate reaction rates

→ No way to measure $S(E)_b$ from direct experiments at energies where screening is important

$S_b(E)$-factor extracted from <u>extrapolation</u> of higher energy data

Indirect Methods for Nuclear Astrophysics

- to measure cross sections at never reached energies (no Coulomb suppression), where the signal is below current detection sensitivity
- to get independent information on U_e
- to overcome difficulties in producing the beam or the target (radioactive ions, neutrons..)

Quite straightforward experiment, no Coulomb suppression, no electron screening but …

Entrance channel

A+a

Several reaction mechanisms link the two channels

Reaction products

C+c+…

The reaction theory is needed to select only one reaction mechanism. However, nowadays powerful techniques and observables for careful data analysis and theoretical investigation.

THM

Basic principle: relevant low-energy two-body σ from quasi-free contribution of an appropriate three-body reaction in quasi free kinematics

$$A + a \rightarrow b + B + s \quad \rightarrow\rightarrow\rightarrow \quad A + x \rightarrow b + B$$

a: x $\oplus$ s clusters

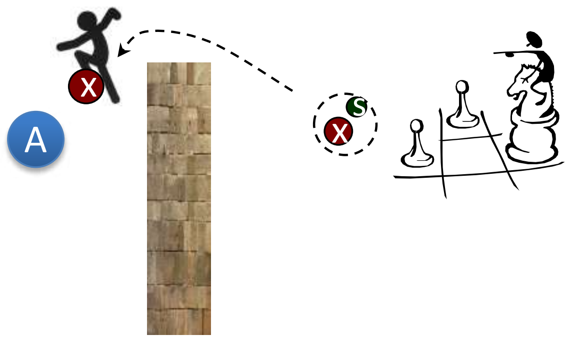

Repulsion wall

Quasi free mechanism

- ✓ only *x* - A interaction
- ✓ *s* = spectator (p_s~0)

$E_A > E_{Coul} \Rightarrow$

<u>NO Coulomb suppression</u>

<u>NO electron screening</u>

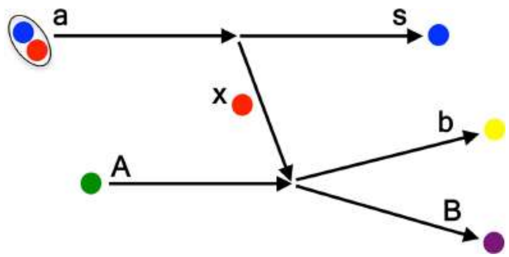

$$E_{q.f.} = E_{Ax} - B_{x\text{-}s} \pm \text{(intercluster motion)}$$

plays a key role in compensating for the beam energy

$$E_{q.f.} \approx 0 \quad !!!$$

THM applied so far to more than 30 reactions, such as ^{6}Li(p,α)^{3}He, ^{7}Li(p,α)α, ^{2}H(d,p)^{3}H, ^{2}H(d, n)^{3}He, ^{10}B(p,α)^{7}Be,^{11}B(p,α)^{8}Be, ^{17,18}O(p,α)^{14,15}N, ^{13}C(α, n)^{16}O, ^{7}Be(n,α)^{4}He, ^{18}F(p,α)^{15}O, ^{19}F(p,α)^{16}O, ^{10}B(p,α)^{7}Be, ^{11}B(p,α)^{8}Be, ^{12}C(^{12}C,α)^{20}Ne, ^{12}C(^{12}C,p)^{23}Na ...

See for review:
R. Tribble et al., Rep. Prog. Phys. **77** (2014) 106901
A. Tumino et al. Ann. Rev. Nucl. Part. Sci. 71 (2021) 346

Theoretical approaches to the THM

$A + a \to c + C + s$ → → → $A + x \to c + C$

PWIA hypotheses:

- beam energy > $a = x \oplus s$ breakup Q-value
- projectile wavelength $k^{-1} \ll x - s$ intercluster distance

$$\frac{d^3\sigma}{d\Omega_B d\Omega_b dE_B} \propto KF \left|\Phi(p_{xs})\right|^2 \left[\frac{d^2\sigma_{xA\to bB}}{dE_{xA} d\Omega}\right]^{HOES}$$

kinematical factor

momentum distribution of *s* inside *a*

Nuclear cross section for the A+x→C+c reaction

MPWBA formalism

(S. Typel and H. Wolter, Few-Body Syst. 29 (2000) 75)

- distortions introduced in the c+C channel, but plane waves for the three-body entrance/exit channel

- off-energy-shell effects corresponding to the suppression of the Coulomb barrier are included

A. Tumino et al., PRL 98, 252502 (2007)

but <u>No absolute value of the cross section</u>

Theoretical approaches to the THM

R. Tribble et al., Rep. Prog. Phys. **77** (2014) 106901

The THM simple factorization can be deduced from the general formula in the case of resonant reactions

Amplitude of the TH reaction

$$M^{\mathrm{PWA(prior)}}(P, \boldsymbol{k}_{aA}) = (2\pi)^2 \sqrt{\frac{1}{\mu_{bB} k_{bB}}}\, \varphi_a(\boldsymbol{p}_{sx})$$
$$\times \sum_{J_F M_F j' l l' m_{j'} m_l m_{l'} M_n} i^{l+l'} \langle j m_j l m_l | J_F M_F \rangle \langle j' m_{j'} l' m_{l'} | J_F M_F \rangle$$
$$\times \langle J_x M_x J_A M_A | j' m_{j'} \rangle \langle J_s M_s J_x M_x | J_a M_a \rangle \, \mathrm{e}^{-\mathrm{i}\delta^{hs}_{bBl}} Y_{lm_l}(-\hat{\boldsymbol{k}}_{bB})$$
$$\times \sum_{\nu,\tau=1}^{N} [\Gamma_{\nu bBjlJ_F}(E_{bB})]^{1/2} [\boldsymbol{A}^{-1}]_{\nu\tau} Y^{*}_{l' m_{l'}}(\hat{\boldsymbol{p}}_{xA})$$
$$\times \sqrt{\frac{R_{xA}}{\mu_{xA}}} [\Gamma_{\nu xAl'j'J_F}(E_{xA})]^{1/2} P_{l'}^{-1/2}(k_{xA}, R_{xA}) (j_{l'}(p_{xA} R_{xA})$$
$$\times [(B_{xAl'}(k_{xA}, R_{xA}) - 1) - D_{xAl'}(p_{xA}, R_{xA})]$$
$$+ 2 Z_x Z_A e^2 \mu_{xA} \int_{R_{xA}}^{\infty} \mathrm{d}r_{xA} \frac{O_{l'}(k_{xA}, r_{xA})}{O_{l'}(k_{xA}, R_{xA})} j_{l'}(p_{xA} r_{xA})).$$

This accounts for:

- HOES effects
- Normalization (very useful for RIBS)

Moreover:
Possible generalization to CDCC & DWBA

However → More complicated!

...for resonant reactions

The A + a(x+s) $\rightarrow$ F*(c + C) + s process is a transfer to the continuum where particle x is the transferred particle

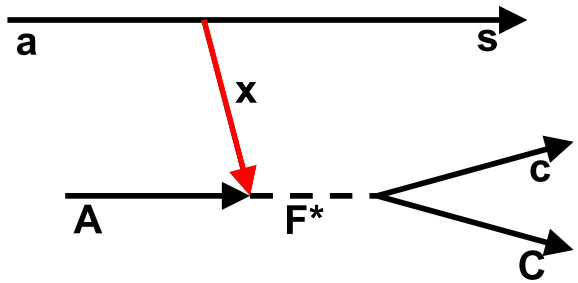

Standard R-Matrix approach cannot be applied to extract the resonance parameters → Modified R-Matrix is introduced instead

In the case of a resonant THM reaction the cross section takes the form

$$\frac{d^2\sigma}{dE_{Cc}\, d\Omega_s} \propto \frac{\Gamma_{(Cc)_i}(E)\, |M_i(E)|^2}{(E - E_{R_i})^2 + \Gamma_i^2(E)/4}$$

$M_i(E)$ is the amplitude of the transfer reaction (upper vertex) that can be easily calculated
→ The resonance parameters can be extracted

When transfer to a bound F state, M^2 is proportional to the ANC of the populated F state

Advantages:

- possibility to measure down to zero energy
- No electron screening
- HOES reduced widths are the same entering the OES S(E) factor (New!)

Reactions studied with the THM.

	Indirect reaction	Direct reaction	References
[1]	$^{2}H(^{7}Li, \alpha\alpha)n$	$^{1}H(^{7}Li, \alpha)^{4}He$	Spitaleri et al 1999, Lattuada et al 2001 [97]
[2]	$^{3}He(^{7}Li, \alpha\alpha)d$	$^{2}H(^{7}Li, \alpha)^{4}He$	Tumino et al 2006 [98]
[3]	$^{2}H(^{6}Li, \alpha^{3}He)n$	$^{1}H(^{6}Li, \alpha)^{3}He$	Tumino et al 2003 [88]
[4]	$^{6}Li(^{6}Li, \alpha\alpha)^{4}He$	$^{2}H(^{6}Li, \alpha)^{4}He$	Spitaleri et al 2001 [22]
[5]	$^{2}H(^{9}Be, \alpha^{6}Li)n$	$^{1}H(^{9}Be, \alpha)^{6}Li$	Wen et al 2008 [99]
[6]	$^{2}H(^{10}B, \alpha^{7}Be)n$	$^{1}H(^{10}B, \alpha)^{7}Be$	Lamia et al 2008, Rapisarda et al 2018, Cvetinovic et al 2018 [100–102]
[7]	$^{2}H(^{11}B, \alpha_0{}^{8}Be)n$	$^{1}H(^{11}B, \alpha)^{8}Be$	Spitaleri et al 2004, Lamia et al 2011 [103,104]
[8]	$^{2}H(^{15}N, \alpha^{12}C)n$	$^{1}H(^{15}N, \alpha)^{12}C$	La Cognata et al 2007 [105]
[9]	$^{2}H(^{18}O, \alpha^{15}N)n$	$^{1}H(^{18}O, \alpha)^{15}N$	La Cognata et al 2009 [106]
[10]	$^{2}H(^{17}O, \alpha^{14}N)n$	$^{1}H(^{17}O, \alpha)^{14}N$	Sergi et al 2010, Sergi et al. 2015 [89,90]
[11]	$^{6}Li(^{3}He, p^{4}He)^{4}He$	$^{2}H(^{3}He, p)^{4}He$	La Cognata et al 2005 [107]
[12]	$^{2}H(^{6}Li, p^{3}H)^{4}He$	$^{2}H(d, p)^{3}H$	Rinollo et al 2005 [108]
[13]	$^{6}Li(^{12}C, \alpha^{12}C)^{2}H$	$^{4}He(^{12}C, ^{12}C)^{4}He$	Spitaleri et al 2000 [109]
[14]	$^{2}H(^{6}Li, t^{4}He)^{1}H$	$n(^{6}Li, t)^{4}He$	Tumino et al 2005, Gulino et al 2010 [110,111]
[15]	$^{2}H(p, pp)n$	$^{1}H(p, p)^{1}H$	Tumino et al 2007, Tumino et al 2008 [112,113]
[16]	$^{2}H(^{3}He, p^{3}H)^{1}H$	$^{2}H(^{2}H, p)^{3}H$	Tumino et al 2011, Tumino et al 2014 [94,114]
[17]	$^{2}H(^{3}He, n^{3}He)^{1}H$	$^{2}H(^{2}H, n)^{3}He$	Tumino et al 2011, Tumino et al 2014 [94,114]
[18]	$^{2}H(^{19}F, \alpha^{16}O)n$	$^{1}H(^{19}F, \alpha)^{16}O$	La Cognata et al 2011, Indelicato et al 2017 [32,115]
[19]	$^{13}C(^{6}Li, n^{16}O)^{2}H$	$^{13}C(\alpha, n)^{16}O$	La Cognata et al 2014 [116]
[20]	$^{2}H(^{18}F, \alpha^{15}O)n$	$^{1}H(^{18}F, \alpha)^{15}O$	Cherubini et al 2015, Pizzone et al. 2016, La Cognata et al. 2017 [92,117,118]
[21]	$^{2}H(^{10}B, \alpha^{7}Li)^{1}H$	$n(^{10}B, \alpha)^{7}Li$	Guardo et al 2019, Sparta et al 2021 [119,120]
[22]	$^{2}H(^{7}Be, \alpha\alpha)^{1}H$	$n(^{7}Be, \alpha)^{4}He$	Lamia et al 2017, Lamia et al 2019, Hayakawa et al 2021 [121–123]
[23]	$^{12}C(^{14}N, \alpha^{20}Ne)^{2}H$	$^{12}C(^{12}C, \alpha)^{20}Ne$	Tumino et al 2018 [30]
[24]	$^{12}C(^{14}N, p^{23}Na)^{2}H$	$^{12}C(^{12}C, p)^{23}Na$	Tumino et al 2018 [30]
[25]	$^{6}Li(^{19}F, p^{22}Ne)^{2}H$	$^{4}He(^{19}F, p)^{22}Ne$	Pizzone et al 2017, Dagata et al 2018 [117,124]
[26]	$^{2}H(^{17}O, \alpha^{14}C)^{1}H$	$^{17}O(n, \alpha)^{14}C$	Oliva et al 2020 [125]
[27]	$^{2}H(^{3}He, pt)^{1}H$	$^{3}He(n, p)^{3}H$	Pizzone et al 2021 [126]
[28]	$^{2}H(^{7}Be, p^{7}Li)^{1}H$	$n(^{7}Be, p)^{7}Li$	Hayakawa et al 2021 [123]
[29]	$^{2}H(^{27}Al, \alpha^{24}Mg)n$	$^{27}Al(p, \alpha)^{24}Mg$	Palmerini et al 2021, La Cognata et al. 2022 [127–129]

12C+12C fusion

C-burning crucial phase in the nucleosynthesis of massive stars (> 8 $M_{\odot}$), determines M_{up}, ignition trigger for superbursts and Type Ia supernovae

astrophysical energy: 1 – 3 MeV

From direct measurement, minimum E: 2.1 MeV

extrapolations differ by 3 orders of magnitude
without inclusion of resonances

Indirect measurement with THM down to 1 MeV:
$^{12}C(^{14}N,\alpha^{20}Ne)^{2}H$ and $^{12}C(^{14}N,p^{23}Na)^{2}H$.
Resonances dominate the astrophysical energy

$^{12}C + ^{12}C \rightarrow \alpha + ^{20}Ne$
$^{12}C + ^{12}C \rightarrow p + ^{23}Na$

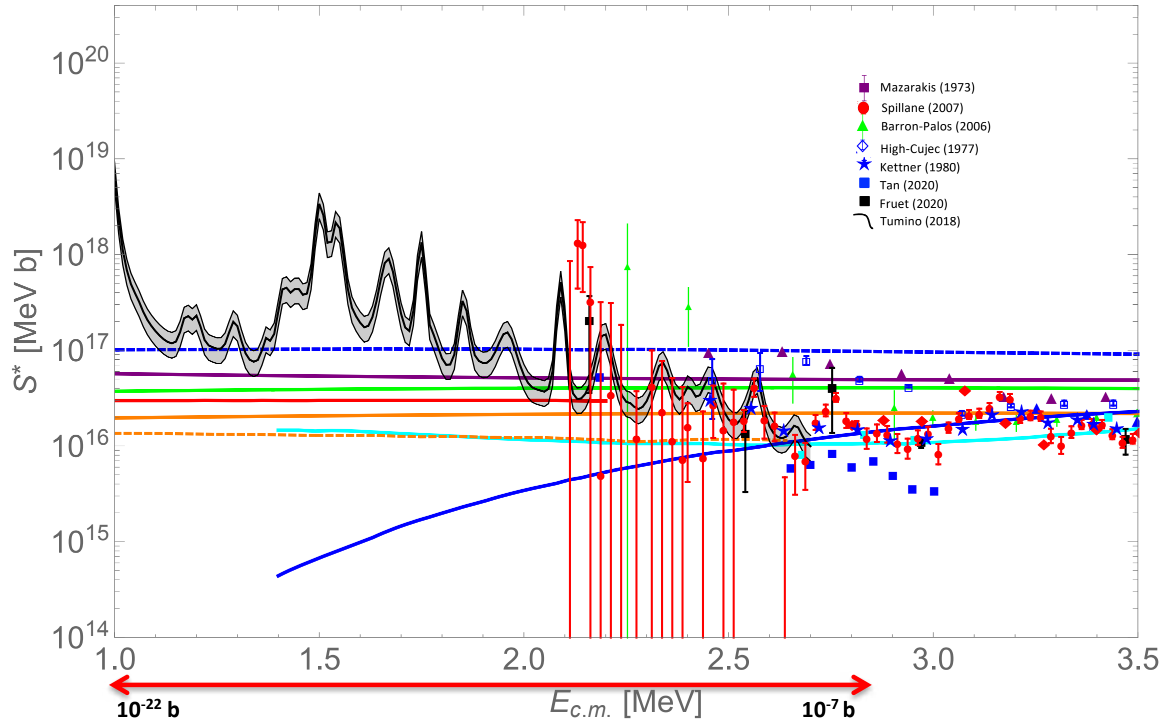

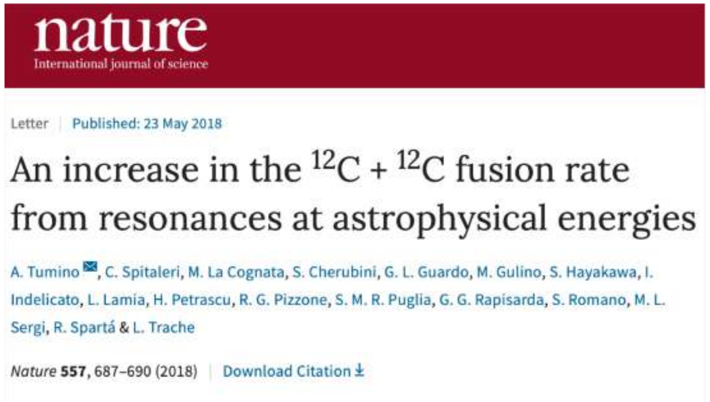

nature
International journal of science

Letter | Published: 23 May 2018

An increase in the $^{12}C + ^{12}C$ fusion rate from resonances at astrophysical energies

A. Tumino, C. Spitaleri, M. La Cognata, S. Cherubini, G. L. Guardo, M. Gulino, S. Hayakawa, I. Indelicato, L. Lamia, H. Petrascu, R. G. Pizzone, S. M. R. Puglia, G. G. Rapisarda, S. Romano, M. L. Sergi, R. Spartá & L. Trache

Nature **557**, 687–690 (2018) | Download Citation

Our Experiment with theTHM

$^{12}C(^{12}C,\alpha)^{20}Ne$ and **$^{12}C(^{12}C,p)^{23}Na$** reactions via the Trojan Horse Method applied to the **$^{12}C(^{14}N,\alpha^{20}Ne)^{2}H$** and **$^{12}C(^{14}N,p^{23}Na)^{2}H$** three-body processes

^{2}H from the ^{14}N as spectator s

Observation of ^{12}C cluster transfer in the $^{12}C(^{14}N,d)^{24}Mg^{*}$ reaction (R.H. Zurmûhle et al. PRC 49 (1994) 5)

E_{14N} =30 MeV> E_{coul} d,p/α coincidence detection

$$E_{QF} = E_{14N}\frac{m_{^{12}C}}{m_{^{14}N}} \cdot \frac{m_{^{12}C}}{m_{^{12}C}+m_{^{12}C}} - 10.27\ \text{MeV}$$

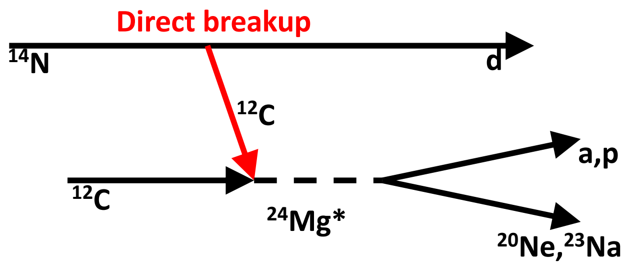

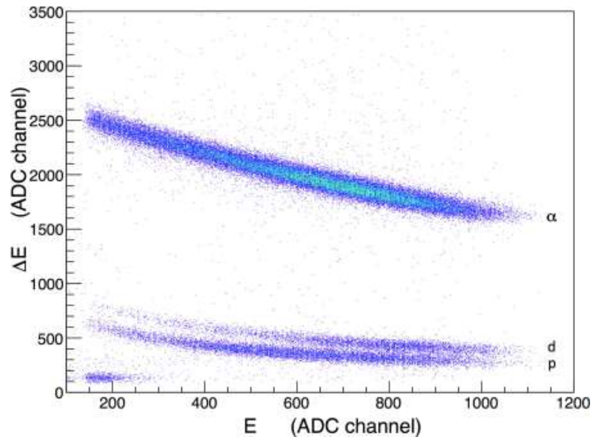

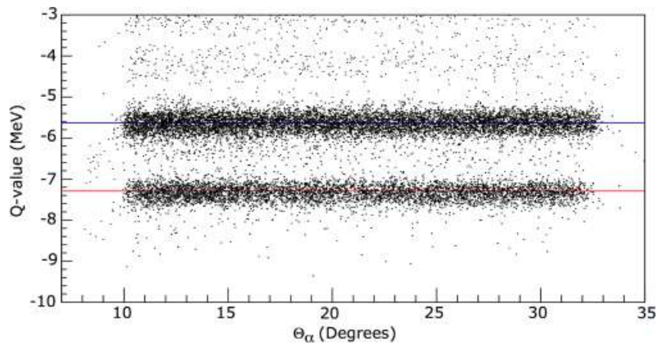

A. Tumino et al., Nature (2018)

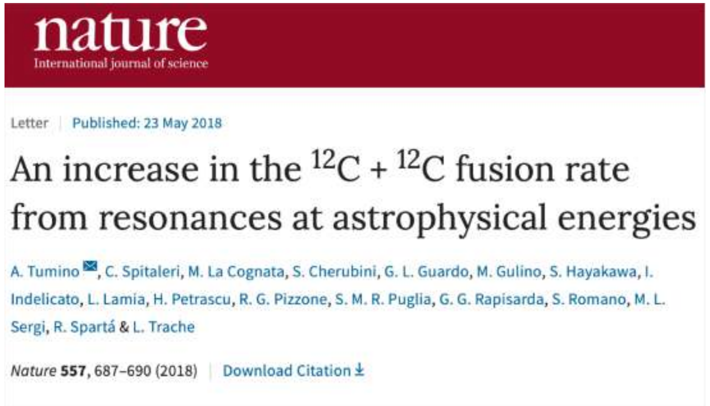
nature
International journal of science

Letter | Published: 23 May 2018

An increase in the $^{12}C + ^{12}C$ fusion rate from resonances at astrophysical energies

A. Tumino, C. Spitaleri, M. La Cognata, S. Cherubini, G. L. Guardo, M. Gulino, S. Hayakawa, I. Indelicato, L. Lamia, H. Petrascu, R. G. Pizzone, S. M. R. Puglia, G. G. Rapisarda, S. Romano, M. L. Sergi, R. Spartá & L. Trache

Nature **557**, 687–690 (2018) | Download Citation

12C+12C Reaction Rate

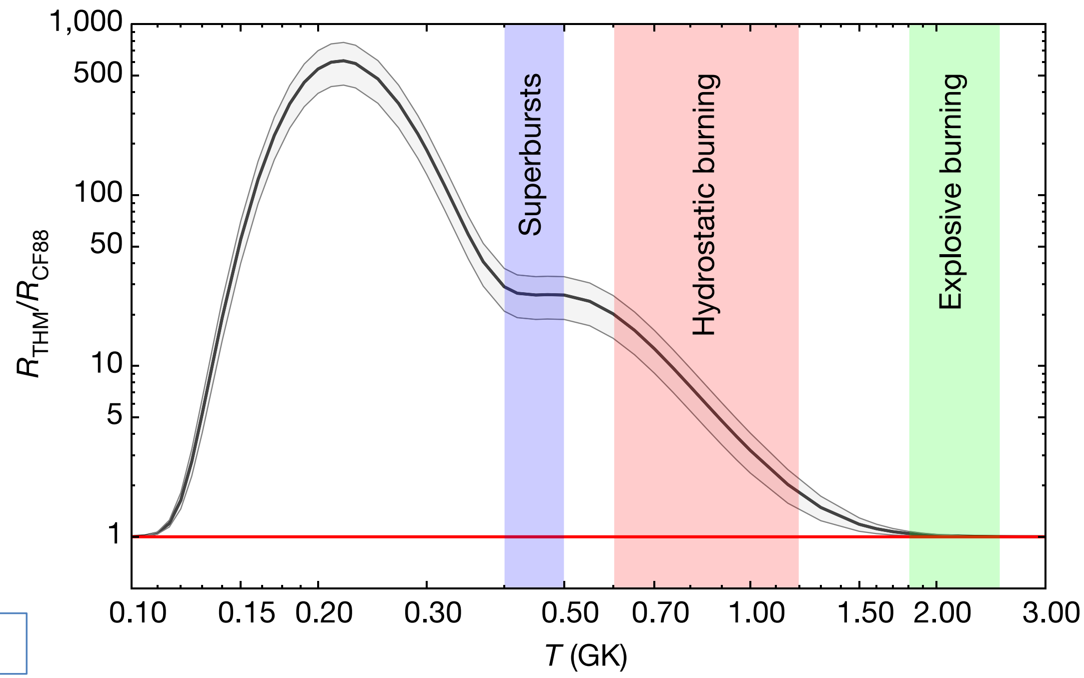

Color shadings mark typical regions for C-burning

Compared to CF88, the present rate increases from a factor of 1.18 at 1.2 GK to a factor of more than 25 at 0.5 GK

12C+16O fusion

- In the late stages of C-burning the abundance of ^{16}O is larger than ^{12}C
  - Ashes of the $^{12}C(\alpha,\gamma)^{16}O$
  - Minor contribution from $^{12}C(^{12}C,2\alpha)^{16}O$
- For $T > 1$GK the rate of the $^{12}C+^{16}O$ fusion starts to be relevant. Principal reactions involved in the process:
  - $^{12}C(^{16}O, \alpha)^{24}Mg$
  - $^{12}C(^{16}O, p)^{27}Al$
  - $^{12}C(^{16}O, n)^{27}Si$

High level density in ^{28}Si. One should see only special states

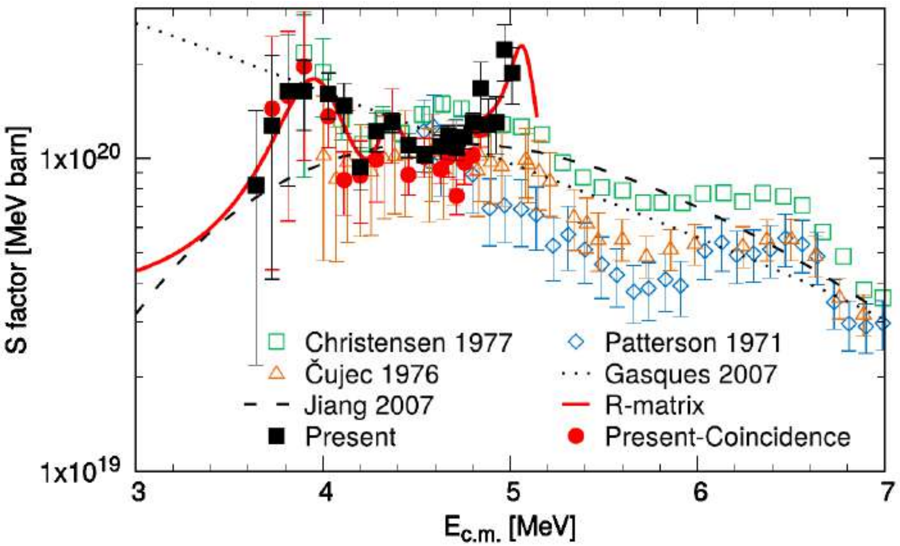

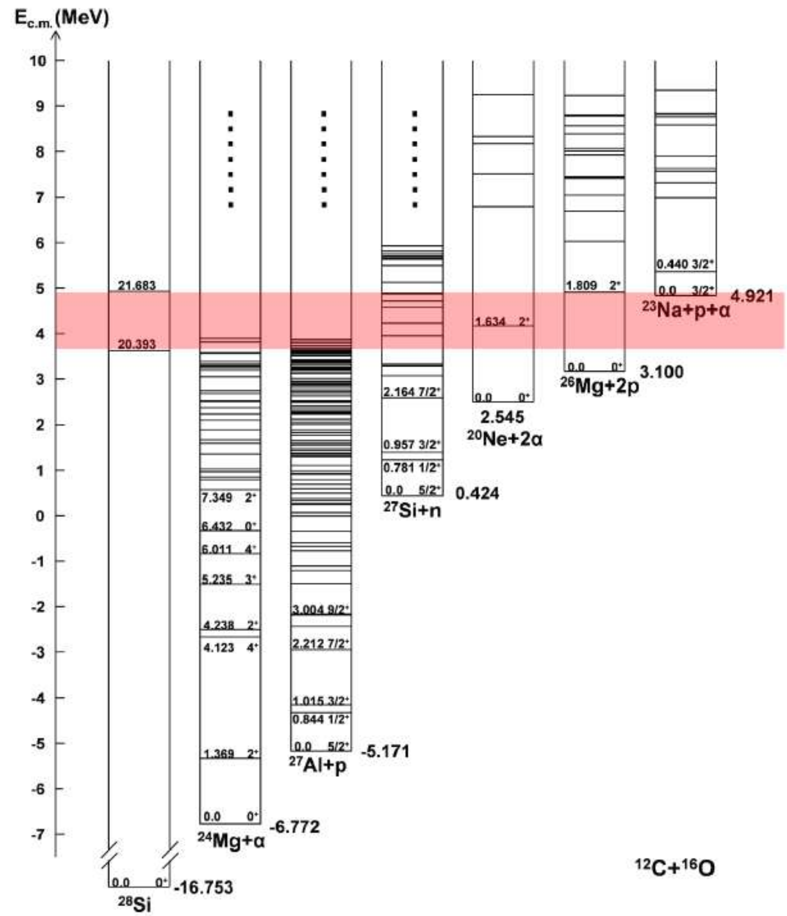

New results with the THM down to 2 MeV, pape in preparation

Charge independence and charge symmetry

After removing the electromagnetic interactions, the NN force between nn, np, pp are almost the same

Charge independence: equality between pp/nn force and np force

Violation: associated to the mass difference between charged and neutral pions

(identical nucleons exchange a neutral pion, a neutron and a proton may exchange both a neutral and a charged pion)

Charge symmetry: equality between pp and nn forces

Charge symmetry breaking: mainly attributed to the up-down quark mass difference

Its validity is supported to some extent by an approximate equality of binding energies of isobar nuclei.

Charge symmetry breaking manifested in the s-wave scattering lengths, a_{NN} that determine the low-energy behavior of NN scattering.

a_{np} directly determined from experiments

a_{pp} not directly accessible from experiments because of Coulomb effects → need to remove them theoretically to reveal the strong interaction contribution to the scattering length

a_{nn} not directly accessible from experiments because of the absence of neutron targets.

… we propose an innovative way to determine a_{pp} →

Two-body cross-section from THM data

THM p-p cross-section from the p+d→p+p+n quasi free reaction

Coulomb effects appear suppressed

Calculated HOES p-p cross section:

$$
\left(\frac{d\sigma}{d\Omega_{\mathrm{c.m.}}}\right)^{\mathrm{HOES}} = \frac{1}{k^2}\Bigg(\frac{1}{4}\Bigg[\Bigg|2\mu_{pp}\, e^2\, e^{-\pi\eta}\Gamma(1+i\eta) \times \left(\frac{(p^2-k^2)^{i\eta}}{(\mathbf{p}-\mathbf{k})^{2(1+i\eta)}} + \frac{(p^2-k^2)^{i\eta}}{(\mathbf{p}+\mathbf{k})^{2(1+i\eta)}}\right) - 2\,T_{CN}(k,\,p)\Bigg|^2\Bigg] + \frac{3}{4}\Bigg[\Bigg|2\mu_{pp}\, e^2\, e^{-\pi\eta}\Gamma(1+i\eta) \times \left(\frac{(p^2-k^2)^{i\eta}}{(\mathbf{p}-\mathbf{k})^{2(1+i\eta)}} - \frac{(p^2-k^2)^{i\eta}}{(\mathbf{p}+\mathbf{k})^{2(1+i\eta)}}\right)\Bigg|^2\Bigg]\Bigg).
$$

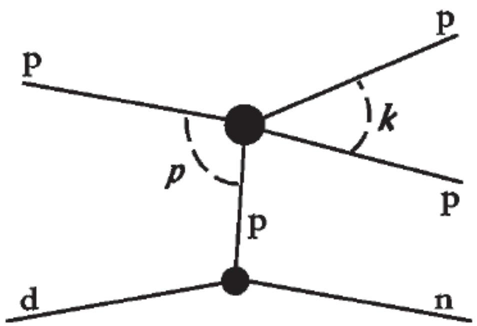

Red line: HOES p-p cross section

Black line: OES p-p cross section

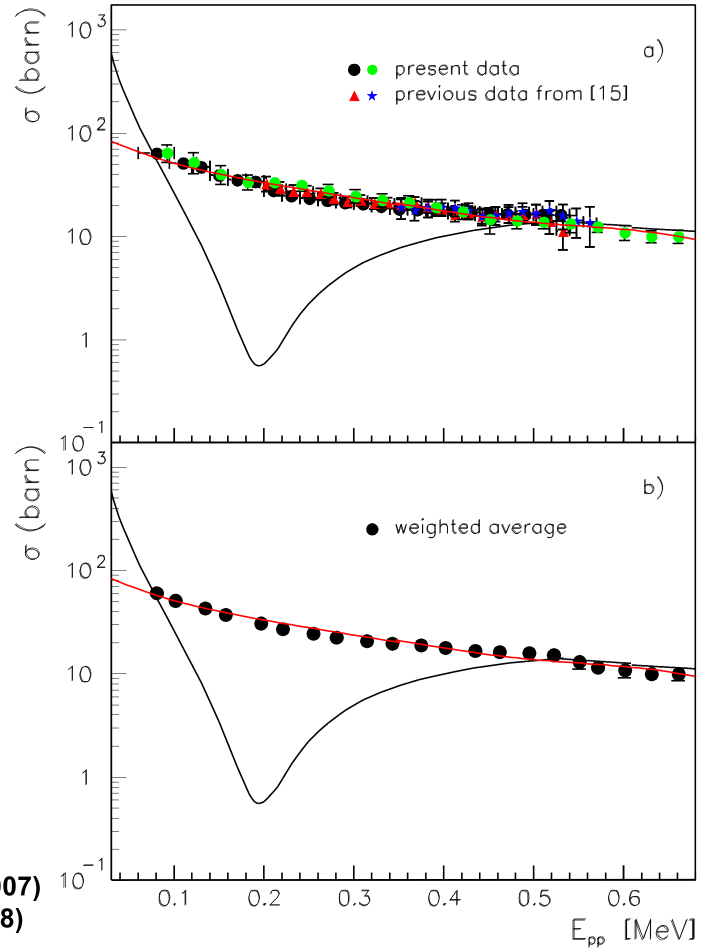

A. Tumino et al. PRL 98, 252502 (2007)

A. Tumino et al. PRC 78, 64001 (2008)

nature > communications physics > articles > article

Article | Open Access | Published: 18 May 2023

Coulomb-free $^1S_0$ $p-p$ scattering length from the quasi-free $p + d \rightarrow p + p + n$ reaction and its relation to universality

Aurora Tumino, Giuseppe G. Rapisarda, Marco La Cognata, Alessandro Oliva, Alejandro Kievsky, Carlos A. Bertulani, Giuseppe D'Agata, Mario Gattobigio, Giovanni L. Guardo, Livio Lamia, Dario Lattuada, Rosario G. Pizzone, Stefano Romano, Maria L. Sergi, Roberta Spartá & Michele Viviani

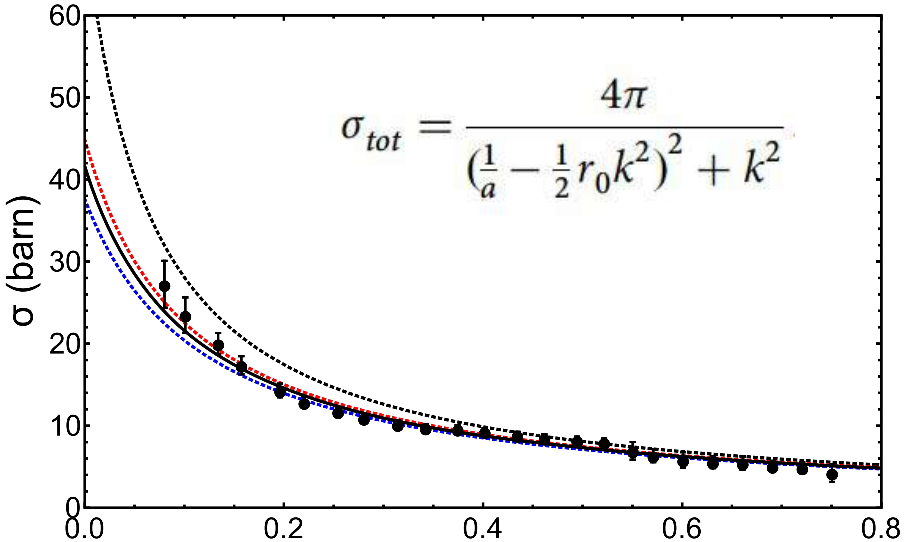

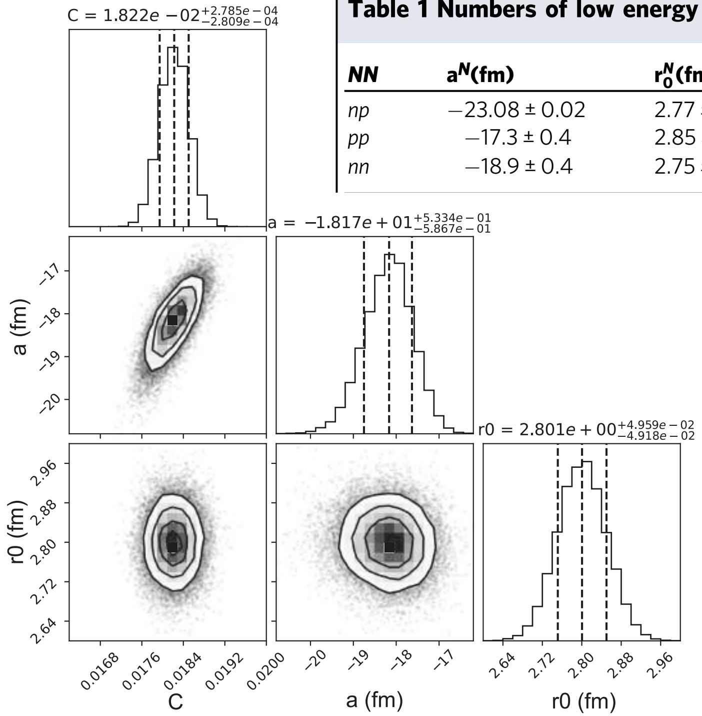

Table 1 Numbers of low energy parameters.

NN	a^N(fm)	r_0^N(fm)	a^{THM}(fm)	r_0^{THM}(fm)
np	-23.08 ± 0.02	2.77 ± 0.05		
pp	-17.3 ± 0.4	2.85 ± 0.04	$-18.17^{+0.53}_{-0.59}$ fm	2.80 ± 0.05 fm
nn	-18.9 ± 0.4	2.75 ± 0.11		

Notice: the NN s-wave phase shift δ contains all short range effects, including the electromagnetic ones. This means that the present analysis of the HOES cross section allows direct access to the short-range p-p interaction as a whole, with its peculiar a_{pp} and r_0 values.

We propose a new paradigm: to assess the charge symmetry breaking of the short-range interaction as a whole, in line with the current understanding that, at a fundamental level, the charge dependence of nuclear forces is due to a difference between the masses of the up and down quark and to electromagnetic interactions among the quarks.

We can exploit universal concepts to better interpret the results, now that Coulomb effects have been removed from the p-p system.

Notably, in the universal window the dynamics is largely independent of the details of the interaction. It is dominated by the long-range behavior allowing for a description based on few parameters.

We construct a two-parameter Gaussian NN interaction with fixed range, valid for s-wave in the spin singlet channel

$$V_{NN}(r) = V_0 e^{-r^2/r_G^2} + \frac{e^2_{NN}}{r}$$

with NN ≡ nn, np, pp and e^2_{p}

the Gaussian form selected to represent the short-range interaction is not relevant, other choices are acceptable as well. Very recently a new calculation using the Eckart potential that exactly represents the S-matrix for the NN system in the universal window (S-matrix is equivalent to the effective range expansion up to the second order):

$$V_{Eck}(\beta, R, r) = -2\frac{\hbar^2}{mR^2}\frac{\beta e^{-r/R}}{(1+\beta e^{-r/R})^2}$$

$$a = 4R\frac{\beta}{\beta-1}$$

$$r_0 = 2R\frac{\beta+1}{\beta}$$

NN	a^N(fm)	r_0^N(fm)	a^{THM}(fm)	r_0^{THM}(fm)	a^{sr}(fm)	r_0^{sr}(fm)
np	-23.08 ± 0.02	2.77 ± 0.05			-23.74± 0.02	2.80 ± 0.08
pp	-17.3 ± 0.4	2.85 ± 0.04	$-18.17^{+0.53}_{-0.59}$	2.80±0.05	-17.9 ± 0.5	2.85 ± 0.09
nn	-18.9 ± 0.4	2.75 ± 0.11			-18.6 ± 0.4	2.85 ± 0.08

A. Tumino, A Kiewsky et al. Few Body Systems 2025

The universal window shows the location of the different NN systems using the numbers here obtained: the coordinates are given by

$[x, y] = [r_0/a_B, r_0/a]$

With a_B given by

$$\frac{1}{a_B} = \frac{1}{a} + \frac{1}{2}\frac{r_0}{a_B^2}$$

From low-energy effective range plus S-matrix pole equation

Interestingly, they lie on the curve $y = x - 0.5x^2$ verifying the correlation as above.

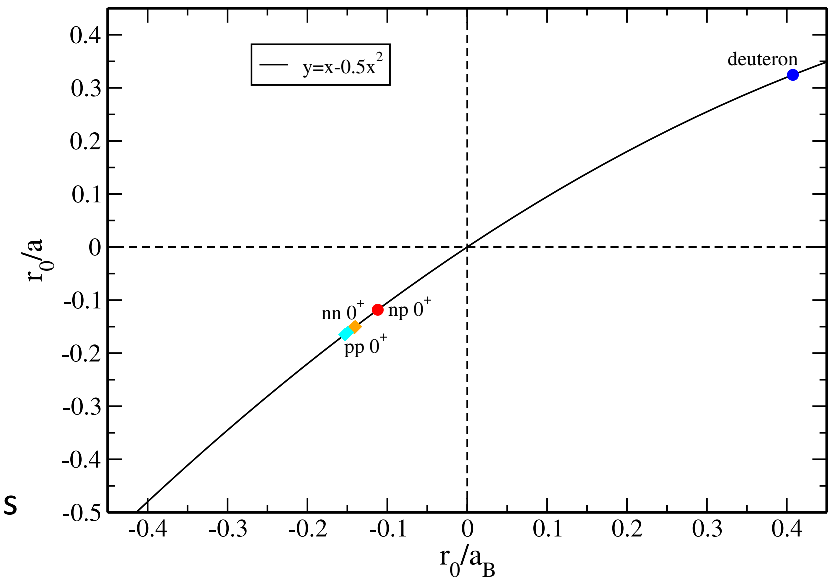

The NN systems are well determined by the corresponding experimental values, and have a precise position along the y(x) curve.

Using the property highlighted here that the systems move along the universal curve, it is possible to reduce the model dependence in the determination of the scattering parameters as produced by the short-range part of the interaction without discriminating between nuclear and electromagnetic.

THM and RIB experiments

RIB experiments: mostly neutron but also p,a induced reactions to tackle the nucleosynthesis beyond Fe

$T > 10^8$ K $\Rightarrow$ $E_0 \sim$ 100 keVs - MeVs $\leq$ E_{coul} → 10^{-6} barn < σ < 10^{-3} barn

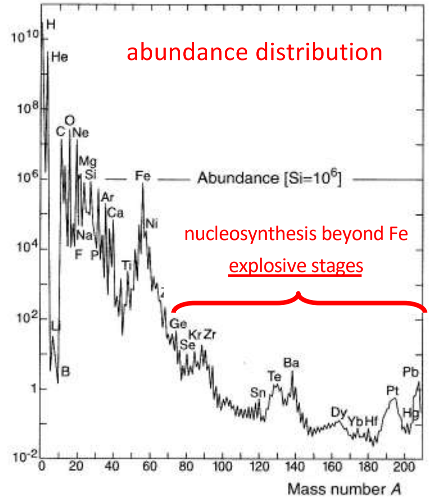

Issues:

- low beam intensities (several o.d.m. lower than for stable beams)
- beam energies usually significantly larger than those needed for astrophysical studies
- changing beam energies in small steps to study the excitation function is often impractical.
- n-targets still under development, low density

THM

- Higher beam energies complying with available RIB facilities
- A single beam energy to study the excitation function → intercluster motion used to cover the astrophysical energy region.
- Use of d-targets (CD_2) as virtual n-targets

very welcome the use of storage rings to overcome beam intensity limitations and improving beam purity at every turn

^{7}Be destruction and the cosmological Li problem

^{7}Li also from primordial ^{7}Be, but in this case need to measure processes that would get rid of ^{7}Be

13. ^{7}Be(n,p)^{7}Li
14. ^{7}Be(n,α)^{4}He
15. ^{7}Be(d,p)2^{4}He

Recent experiment: ^{7}Be(n,a)^{4}He down to E_{cm} ~ 20 keV via ^{7}Be(d,a^{4}He) ^{1}H

EXOTIC facility
E_Beam=20.4 MeV, purity ~ 99 %
i ~5-8 10^{5} pps, beam spot of ~ 9 mm

Another experiment @ CRIB to also measure the ^{7}Be(n,$p_{0,1}$)^{7}Li
E_Beam=22.2 MeV, purity ~ 99 %
i ~ 10^{6} pps, beam spot of ~ 9 mm

Role of ^{7}Be clear only after systematic measurements of all relevant reactions

Influence on primordial ^{7}Li abundance of about 10%
Potential influence also from 7Be(d,) and 7Be(t,)

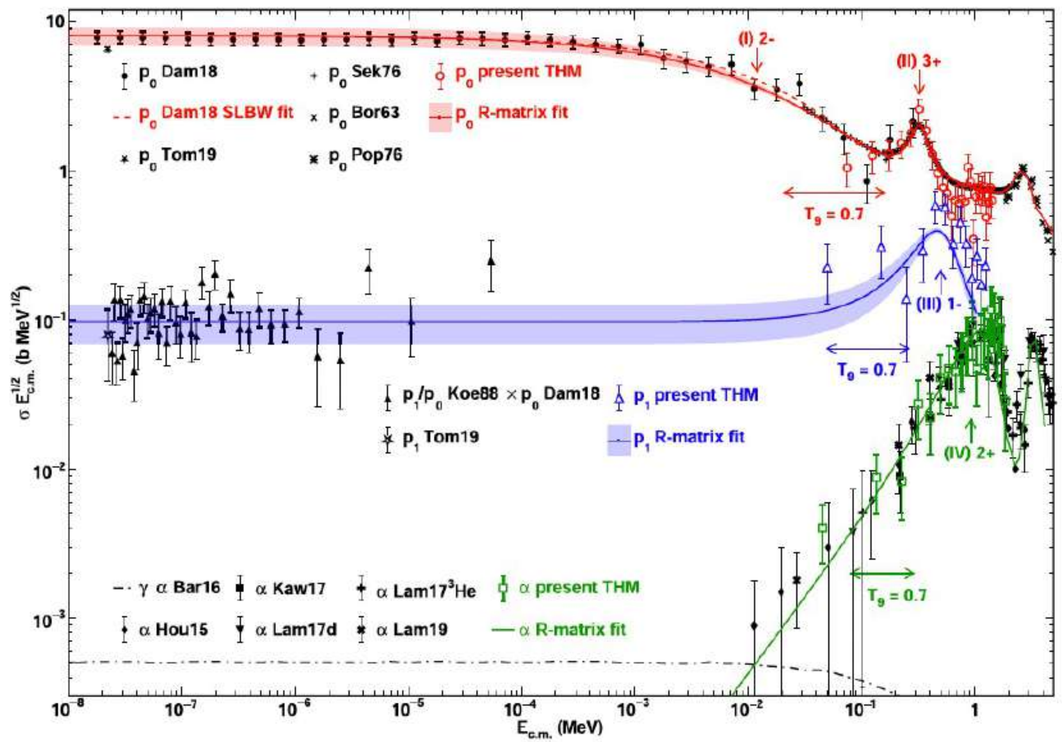

S. Hayakawa et al, Astrophysical Journal Letters 915 (2021) L13

Conclusions

Nuclear physics is a fundamental pillar of Nuclear Astrophysics

Indirect methods are unique tools to investigate reactions on energy ranges difficult to study otherwise

Still great potential for future applications (also beyond astrophysical applications)

Thank you for your attention!